



## Research on diatomite from Polish deposits and the possibilities of its use

J. Marczyk, K. Pławecka, M. Hebdowska-Krupa, M. Nykiel, M. Łach \*

Chair of Material Engineering and Physics, Cracow University of Technology,  
Jana Pawła II 37, 31-864 Cracow, Poland

\* Corresponding e-mail address: [michal.lach@pk.edu.pl](mailto:michal.lach@pk.edu.pl)

ORCID identifier:  <https://orcid.org/0000-0001-5713-9415> (M.Ł.)

### ABSTRACT

**Purpose:** Diatomite from a deposit in Jawornik Ruski (Poland) has been selected as the material for study. The paper aimed to show the possibility of using diatomite from the Carpathian Foothills as a sorbent of petroleum substances.

**Design/methodology/approach:** Diatomite in the delivery condition (DC) and diatomite after calcination were used for this study. The material was calcined at 600, 650, 750, 850 and 1000°C. The diatomaceous earth was then granulated. The morphology of diatomite was observed using SEM. Particle size distribution was determined by Laser Particle Analyzer, chemical composition was determined by XRF, and mineralogical composition by XRD. Specific surface area, pore volume and pore size were determined. Thermal analysis (TG, DTA) was carried out. Absorption capacity tests were performed and the effect of diatomite addition on water absorption of concrete samples was determined.

**Findings:** Within the framework of the study, it was shown that diatomite from the Jawornik deposit could be successfully used as a sorbent for petroleum substances. The absorption capacity of calcined at 1000°C diatomaceous earth was 77%. The obtained result exceeds the effectiveness of previously used absorbents, for which the sorption level is 60-70%. This allows commercial use of diatomite from deposits in Poland. In addition, water absorption tests have shown that diatomaceous earth can successfully replace cement used in concrete production. The most favourable effect on the reduction of water absorption is the addition of diatomite in the amount of 10%.

**Practical implications:** The properties of diatomaceous earth from the Jawornik Ruski deposit indicate its high potential for use in the synthesis of geopolymers, which is important not only from an economic but also from an ecological point of view.

**Originality/value:** The novelty of this work is the demonstration of the possibility of using diatomite as a sorbent of petroleum substances with high efficiency, exceeding the previously used sorbents.

**Keywords:** Amorphous materials, Diatomite, Sorption of petroleum substances, Water absorption

**Reference to this paper should be given in the following way:**

J. Marczyk, K. Pławecka, M. Hebdowska-Krupa, M. Nykiel, M. Łach, Research on diatomite from Polish deposits and the possibilities of its use, *Journal of Achievements in Materials and Manufacturing Engineering* 115/1 (2022) 5-15. DOI: <https://doi.org/10.5604/01.3001.0016.2337>

### MATERIALS



## 1. Introduction

Diatomaceous earth (otherwise known as diatomite) is a fine-grained, friable siliceous sedimentary rock of light colour and a chemical formula of  $\text{SiO}_2 \cdot n\text{H}_2\text{O}$  [1,2]. It consists of the skeletal remains of single-celled aquatic plants (algae), called frustules, which belong to the diatom class Bacillariophyceae of the genus Bacillariophyta [3-5]. Diatom skeletons are iridescent or amorphous hydrated silica. They may also contain mica group minerals (muscovite) and a small content of clay minerals such as kaolinite, illite and organic matter [6].

The silica contained in diatomite is amorphous and reactive. For this reason, diatomite rocks have good pozzolanic properties and can be perfectly suitable as a cement additive [1]. Due to its low density and low thermal conductivity, and at the same time, high inertness, surface area, porosity and high absorption capacity, diatomite is a material well suited for industrial applications [7-9]. Its properties favour its use as an absorbent, filtration, thermal insulation material and as a catalyst carrier [6, 10-12]. Diatomite is characterized by parameters conducive to its use for environmental purification and elimination of pollution by heavy metal ions and cationic dyes [13,14]. It can also serve as a reinforcing filler for polymers [15].

Diatomite deposits are found worldwide in many countries, including the USA, Canada, Brazil, Japan, Germany, Denmark, Belgium, Iceland, France, Algeria, Spain, Italy, Morocco and Cyprus [16]. In Poland, an active open-pit diatomite mine is located in the Eastern Carpathians, in Podkarpackie Voivodeship, within the Menilite series and Krosno strata, in Jawornik Ruski. Diatomite derived from Tertiary formations has a density of  $1.42 \text{ g/cm}^3$  and an average porosity of about 28.5%. Diatomite production from the deposit in Jawornik Ruski deposit in 2018 amounted to 0.58 thousand tons [8]. The domestic producer of diatomite raw materials is Specialized Mining Company GÓRTECH Sp. z o.o in Cracow.

Research commissioned by the owner of the mine - Specialized Mining Company GÓRTECH Sp. z o.o. and carried out by the Professional Radiesthesia Laboratory "GEOBIOTRONIKA" has shown that diatomite can be used to neutralize the negative effects of geopathic (terrestrial) radiation in the B-S-Pc range of the radiesthesia spectrum. Diatomite has a selective effect, as it does not suppress the natural positive radiation bands in the Cz-UF range for humans and animals. As research has shown, diatomite, in addition to neutralizing the effects of geopathic radiation, has extremely valuable properties from the point of view of ecological construction, namely: biological and chemical neutrality, thermal resistance up to  $1000^\circ\text{C}$ , non-

flammability, neutrality for human health, high compressive strength – of the order of 3.0 MPa, good insulating properties and lightness.

It is possible to use diatomite, for example, as an aggregate when making spouts. A diatomite-based spout can provide a screen that effectively reduces negative geopathic radiation and can contribute to the well-being and health of humans and animals.

Research by Li et al. [17] shows that it is also possible to use diatomite as a PCM (phase change materials) storage material. Due to its oil-absorbing properties, diatomite can also be a material that absorbs large amounts of paraffins, which are phase-change materials. In studies, it has been proven that after surface modification, diatomite can absorb paraffins and be used in concrete mixtures.

Another application of diatomite can be 3D biocomposites based on polyurethanes [18]. Studies conducted using diatomite and hydroxyapatite as polyurethane reinforcements have shown that composites with diatomite have better thermal resistance than biocomposites with hydroxyapatite. Turkten [19] presented the developed  $\text{CeO}_2$ -diatomite composites with high photocatalytic performance, which be used to remove pollutants from water.

The addition of diatomite can also have a positive effect in geopolymer mortars as a replacement for fly ash. A study [20] showed that the addition of diatomite improves the workability of mortars (while it may reduce compressive strength). However, studies show that compared to colloidal silica, adding diatomite can improve the compressive strength of geopolymers [21]. Importantly, the addition of diatomite to geopolymers can have a positive effect on reducing the thermal conductivity coefficient [22]. It has been proven that it is possible to use recycled diatomite for geopolymer binders – after being used by the brewing and wine industries [23].

Also, it is possible to replace part of the cement with diatomaceous earth in concretes. The results of studies [24] show that diatomite material can be used as a replacement for cement up to 40% without significant loss of compressive strength, along with improved tensile strength and transport properties of cement mortars in later maturation periods. Whereas Fang et al. [25] showed that diatomite could be used to modify coastal cement soil. The results showed that the addition of diatomite improves the mechanical properties of soil cement.

This paper aims to demonstrate the applicability of diatomite from the Carpathian Foothills. In the study, original solutions for the material diatomite earth from the Jawornik Ruski mine are presented by means of absorption capacity and water absorption tests.

## 2. Materials and methodology of research

### 2.1. Materials

The material for the study is diatomite from the Carpathian Foothills, which occurs within Tertiary formations. The deposit is located in the Leszczawka region of the Podkarpackie Voivodeship in Jawornik Ruski (producer: GÓRTECH Sp. z o.o., Cracow, Poland). The physical and chemical properties of the material were determined by the producer in accordance with the standard BN-91/0568-01 [26]: moisture – max. 6%, SiO<sub>2</sub> – min. 69%, Al<sub>2</sub>O<sub>3</sub> – max. 11.8%, Fe<sub>2</sub>O<sub>3</sub> – approx. 4.3%, pH – from 5.7 to 8.3, bulk density (for 0.5-3 mm) – 900 g/l, grey.

The diatomaceous earth was calcined at 600°C, 650°C, 750°C, 850°C and 1000°C. The material was then granulated in a drum granulator. Diatomite with a granulation of 0.5-3 mm was used for the study.

### 2.2. Methods

Detailed observations of the particle morphology of diatomite in the raw state were made using a scanning electron microscope JEOL IT200 (JEOL, Tokyo, Japan).

Particle size analysis was carried out using an Anton-Paar PSA 1190LD particle size analyzer (Anton-Paar, Graz, Austria, 2021). Particle size analysis was performed on diatomite pellets of 0.5-3 mm.

The chemical composition of calcined diatomite was studied on a SPECTRO AMETEK X-ray fluorescence spectrometer (AMETEK, Inc., Germany).

The mineralogical composition of diatomite was investigated by means of an X-ray diffraction method using a PANalytical Aeris (Malvern Panalytical, Almelo, Netherlands) diffractometer. Diffractograms were recorded using Cu-K $\alpha$  radiation in the scan range of 10-100°(2 $\theta$ ), and with a step size of 0.003°(2 $\theta$ ). The quantitative analysis of diatomite was carried out using the Rietveld method.

The tests of specific surface area, pore volume and pore diameter were carried out using a Quantachrome Autosorb iQ-MP physical sorption analyzer (Anton Paar, Graz, Austria). The sample degassing process was carried out in several stages: 1/ heating to the degassing temperature of 80°C at the rate of 2°C/min with soaking time of 30 minutes; 2/ heating to 120°C at the rate of 2°C/min and soaking for 30 minutes; 3/ heating to degassing temperature of 350°C at the rate of 5°C/min and soaking time of 300 minutes. The single-point, and multi-point Brunauer-Emmett-Teller (BET) method determined the specific surface area. The pore volume and pore diameter were determined by the BJH method (Barrett-Joyner-Halenda). The microporosity of the

samples was determined using the Dubinin-Raduszkiewicz (DR) method. The results were analyzed with Quantachrome ASiQwin software.

Differential Thermal Analysis (DTA), coupled with Thermogravimetry (TG), was performed with NETZSCH STA 409 C/CD instrument (Netzsch GmbH, Selb, Germany). The samples were heated at 10°C/min. The tests were carried out in the temperature range from 30°C to 1000°C in an argon atmosphere. Comprehensive testing on an advanced thermal analyser was aimed at selecting the optimum calcination temperature.

The absorption capacity of diatomite aggregate with a grain gradation of 0.9-0.4 mm (Kr-0.9-0.4) in terms of petroleum substances was tested using the Westinghouse method. The aggregate was tested in its delivered condition and after calcination at temperatures: 600°C, 650°C, 750°C, 850°C and 1000°C. The tests were carried out on diesel fuel, meeting the requirements of the Polish standard PN-EN 590 on diesel fuel grades for temperate climates. A schematic of the test stand is presented in Figure 1.

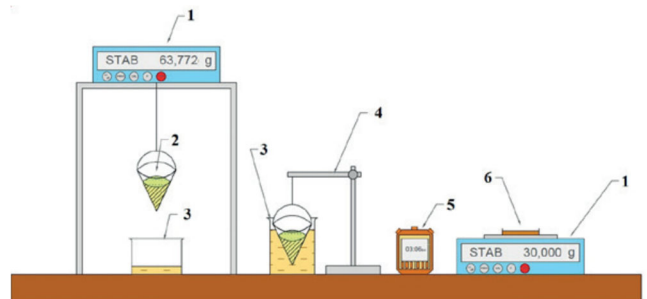


Fig. 1. Scheme of the test stand: 1) analytical balance, 2) conical grid (sieve), 3) beaker with test medium, 4) tripod, 5) stopwatch, 6) Petri dish [27]

C16/20 concrete samples with 0%, 10% and 20% wt. diatomite were prepared for the water absorption tests. Diatomite in the delivery condition (DC) and calcined diatomite at 850°C were used. Tests were carried out on samples of 50×50×50 mm and 150×150×150 mm. The chemical composition of the prepared samples is shown in Table 1.

## 3. Results

### 3.1. Microstructure observations

Figure 2 shows the morphology of diatomaceous earth particles in the raw state. The identified species are typical skeletal forms, mainly discoid frustules of the

Thalassiosiraceae family, occurring in the form of tubes with holes [8]. Remains of diatoms can be seen. Diatoms are characterized by a complex, highly microporous structure with numerous pores, cavities and channels. As a result, they

can have a large specific surface area and high absorption properties. Diatomite with such properties can find application as an adsorption material for filtration [5].

Table 1.  
Composition of samples prepared for water absorption tests

Designation	Composition, g					
	Cement	Sand	Aggregate	Water	Diatomite	Type of diatomite
16/20C	200	400	750	120	–	–
16/20C+20%DC	200	400	750	120	40	delivery condition (DC)
16/20C+10%DC	200	400	750	120	20	delivery condition (DC)
16/20C+20%850°C	200	400	750	120	40	calcined at 850°C
16/20C+10%850°C	200	400	750	120	20	calcined at 850°C

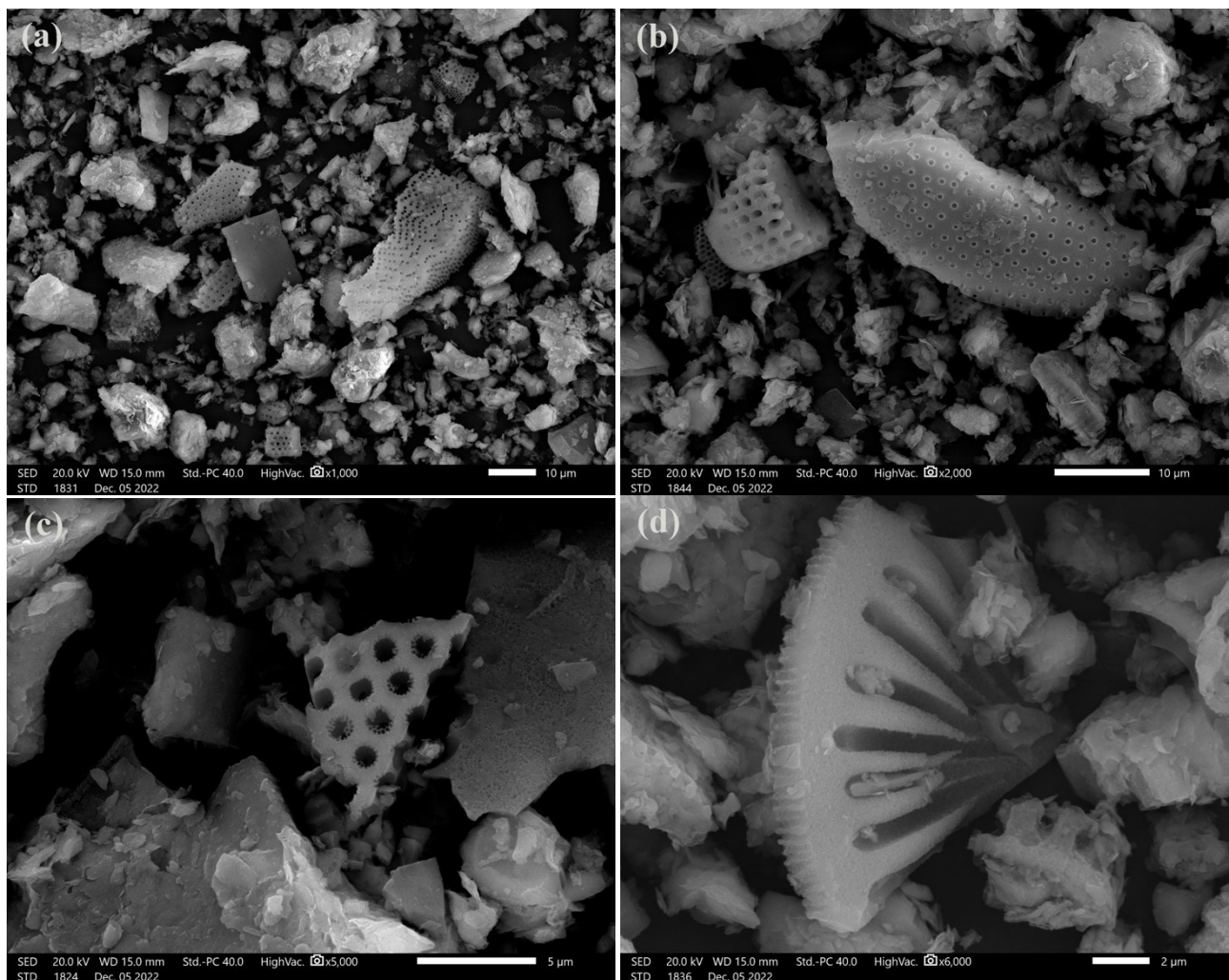


Fig. 2. Morphology of diatomite particles (in delivery condition (DC)): (a) remains of diatom frustules, (b) discoid frustules of the Thalassiosiraceae family in the form of tubes with holes on the outer wall, (c) a flat diatom debris resembling a plate, (d) a flat circular diatom particle with radial symmetry and radial dimples



### 3.2. Particle size distribution

Figure 3 and Table 2 show the results of the particle size distribution for diatomite with granulation of 0.5-3 mm.

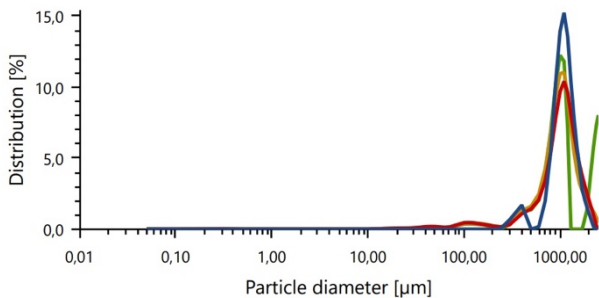


Fig. 3. Particle size distribution of granular diatomite

Table 2.  
Particle size distribution of granular diatomite

	Mean value, $\mu\text{m}$
$D_{10}$	$461.583 \pm 158.342$
$D_{50}$	$960.914 \pm 52.126$
$D_{90}$	$1675.738 \pm 360.934$
Mean size	$1048.427 \pm 49.120$
Span	$1.282 \pm 0.526$

The granular diatomite particle size distribution was relatively narrow (span = 1.282). 10% of the particles ( $D_{10}$ ) have a diameter of less than 461.583  $\mu\text{m}$ , 50% of the particles ( $D_{50}$ ) have a diameter of 960.914  $\mu\text{m}$ , while 90% of the particles ( $D_{90}$ ) have a diameter of less than 1675.738  $\mu\text{m}$ . Diatomite of this size is commonly used for industrial-scale absorption applications.

### 3.3. Chemical composition

Table 3 shows the chemical composition of diatomite after the calcination process at 750°C.

The predominant constituent of calcined diatomite is  $\text{SiO}_2$ , occurring at 81.57%. Such a high content corresponds to silica polymorphs (such as quartz) and aluminosilicate minerals [1]. In the studied material, aluminium oxide occurs in a high proportion of 11.01%, which may be due to the presence of kaolinite [6]. Iron oxide was also detected at 3.571%. The sum of acidic oxides ( $\text{SiO}_2$ ,  $\text{Al}_2\text{O}_3$ ,  $\text{Fe}_2\text{O}_3$ ) exceeded 80%, suggesting their high potential for using the material in the synthesis of geopolymers [23]. Calcined diatomite contains a small number of impurities, such as  $\text{K}_2\text{O}$ ,  $\text{MgO}$ ,  $\text{Na}_2\text{O}$ ,  $\text{CaO}$ ,  $\text{P}_2\text{O}_5$ , among others. A high content of trace elements was revealed. The highest proportion was

Table 3.

Chemical composition of calcined diatomite (at 750°C)

Element	Concentration	Unit
$\text{Na}_2\text{O}$	0.505	%
$\text{MgO}$	1.045	
$\text{Al}_2\text{O}_3$	11.01	
$\text{SiO}_2$	81.57	
$\text{P}_2\text{O}_5$	<0.0048	
S	0.06369	
$\text{SO}_3$	0.1590	
Cl	<0.00016	
$\text{K}_2\text{O}$	1.906	
CaO	0.4044	
Fe	2.498	$\mu\text{g/g}$
$\text{Fe}_2\text{O}_3$	3.571	
$\text{TiO}_2$	5258	
$\text{V}_2\text{O}_5$	200.2	
$\text{Cr}_2\text{O}_3$	184.3	
MnO	257.1	
CoO	<17	
NiO	49.5	
CuO	75.3	
ZnO	85.2	
Ga	8.6	
$\text{As}_2\text{O}_3$	12.2	
Se	<1.0	
Br	<1.0	
$\text{Rb}_2\text{O}$	103.7	
SrO	61.7	
Y	19.4	
$\text{ZrO}_2$	166.5	
$\text{Nb}_2\text{O}_5$	6.8	
MoO	<1.2	
Ag	–	
Cd	<2.4	
In	<1.8	
$\text{SnO}_2$	<3.4	
$\text{Sb}_2\text{O}_5$	<3.8	
Te	<4.2	
I	<11	
Cs	<10	
BaO	273.5	
$\text{La}_2\text{O}_3$	22.5	
$\text{Ce}_2\text{O}_3$	34.9	
$\text{Ta}_2\text{O}_5$	<4.8	
$\text{WO}_3$	<2.0	
Hg	<1.0	
Tl	<1.0	
Pb	8.1	
Bi	<1.0	
Th	4.1	
U	<1.7	

recorded for TiO<sub>2</sub> (5258 µg/g), BaO (273.5 µg/g), MnO (257.1 µg/g), V<sub>2</sub>O<sub>5</sub> (200.2 µg/g), Cr<sub>2</sub>O<sub>3</sub> (184.3 µg/g), ZrO<sub>2</sub> (166.5 µg/g), Rb<sub>2</sub>O (103.7 µg/g), ZnO (85.2 µg/g), CuO (75.3 µg/g) and SrO (61.7 µg/g). The content of other trace elements does not exceed 50 µg/g.

The Si/Al ratio and the share of mineral impurities in natural and calcined diatomite may differ slightly. Comparing the chemical composition of diatomite before calcination (based on the values provided by the producer) and after treatment, it can be observed that the Si/Al ratio increases with the calcination temperature. Chaisena et al. [28] in their work noticed that the Si/Al ratio of diatomite increases as the treatment temperature increases to 1000°C. They also observed an increased share of SiO<sub>2</sub>, Al<sub>2</sub>O<sub>3</sub>, Fe<sub>2</sub>O<sub>3</sub>, MgO and TiO<sub>2</sub> after diatomite calcination at temperatures of 900°C-1100°C.

### 3.4. Analysis of mineralogical composition

Figure 4 shows the X-ray diffraction pattern for diatomite with granulation of 0.5-3 mm. The results of the quantitative analysis are shown in Table 4.

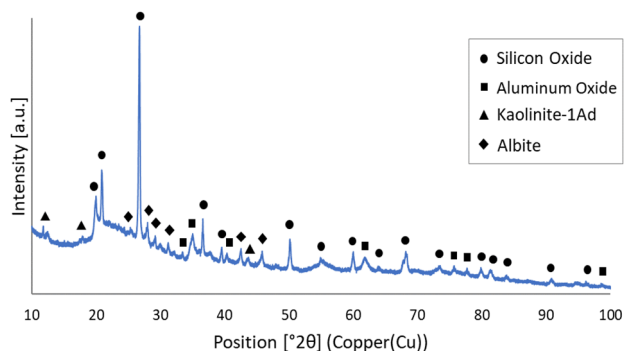


Fig. 4. XRD pattern of granular diatomite 0.5-3 mm

Table 4. Qualitative and quantitative X-ray analysis of diatomite

Phase	Chemical formula	Share, %
Silicon Oxide	SiO <sub>2</sub>	23.4
Aluminum Oxide	Al <sub>2</sub> O <sub>3</sub>	0.5
Kaolinite-1Ad	Al <sub>2</sub> Si <sub>2</sub> O <sub>5</sub> (OH) <sub>4</sub>	54.7
Albite	NaAlSi <sub>3</sub> O <sub>8</sub>	21.5

The broad X-ray diffraction pattern of the diatomite indicates that it is an amorphous material [10]. The presence of a kaolinite phase (ref. code: 01-075-1593) was detected in the diatomite in an amount of 54.7%, as confirmed by reflections mainly at  $2\theta = 11.73; 17.56; 43.39$ . The material also showed the presence of quartz (ref. code: 01-079-6238)

and albite (ref. code: 00-009-0466) in similar percentages of 23.4% and 21.5%, respectively. Aguilar-Mamani et al. [29], in their work, also demonstrated the presence of quartz and albite phases for the XRD pattern of diatomaceous earth. Traces of aluminium oxide (ref. code: 04-004-5291) were also detected at  $2\theta = 33.12; 61.94; 77.61$ .

Mineralogical analysis of diatomite by Figarska-Warchoł et al. [30] also showed the presence of quartz, kaolinite and albite reflections. They report that diatom shells are composed of amorphous silica.

### 3.5. Determination of specific surface area and porosity

Figure 5 shows the nitrogen adsorption-desorption isotherms of delivery condition (DC) diatomite and calcined diatomite at 650°C, 850°C and 1000°C.

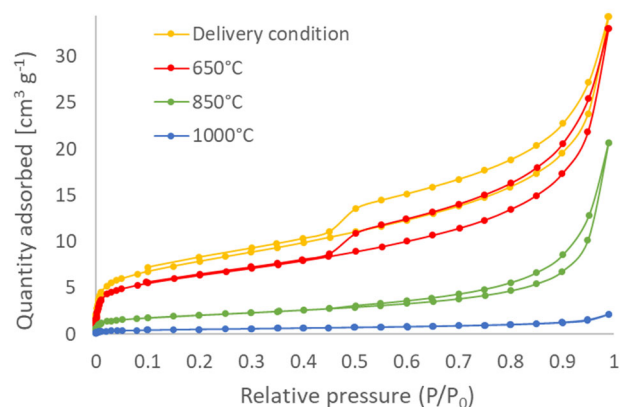


Fig. 5. Adsorption-desorption isotherms of nitrogen for diatomite in the delivery condition and calcined diatomaceous earth at 650°C, 850°C and 1000°C

The shape of the adsorption isotherms depends on the pore size as well as on the intensity of the adsorbate-adsorbent interaction [31]. According to the IUPAC classification, all the presented N<sub>2</sub> sorption isotherms represent the type IV isotherm, which is characteristic of mesoporous materials [32]. In the obtained isotherms, there is an H3-type hysteresis loop. The presence of mesopores in the material may be due to the fact that the isotherms had a larger hysteresis loop at higher relative pressure ( $P/P_0$ ) [33].

Table 5 shows the results of the porous texture analysis of diatomite.

It was observed that the specific surface area of diatomaceous earth decreases as the calcination temperature increases. The highest specific surface area of the material is in the delivery condition (about 27 m<sup>2</sup>/g). Using a temperature

of 650°C, the specific surface area decreased by about 19%. A surface area of about 22 m<sup>2</sup>/g was obtained. After calcination at 850°C, the specific surface area of diatomite decreased by 74% and was about 7 m<sup>2</sup>/g. Moreover, the use of a calcination temperature of 1000°C resulted in a decrease in the specific surface area by as much as 93%, giving a result of less than 2 m<sup>2</sup>/g. As the calcination temperature increased, the pore volume and size decreased.

Table 5.  
Porous texture analysis of diatomite

Texture parameters		Sample No.			
		DC	650°C	850°C	1000°C
Specific surface area, m <sup>2</sup> /g	BET (Single)	26.545	21.624	6.969	1.767
	BET (Multi)	27.970	22.479	7.357	1.930
Pore volume, cm <sup>3</sup> /g	Total P/P <sub>0</sub> =0.99	0.053	0.051	0.032	0.003
	BJH	0.050	0.049	0.031	0.003
	DR	0.011	0.009	0.003	0.001
Pore size, nm	BJH	1.692	1.694	1.690	1.691
	DR	1.987	1.984	1.872	1.679

Xiao et al. [34] noted that the specific surface area of diatomite after calcination increased and reached a maximum of 600°C. Then, the specific surface area decreased in the temperature range from 600°C to 900°C. The increase in the specific surface area up to 600°C may have been due to the removal of impurities from the micropores.

In general, the mechanism for the decrease in specific surface area may change with temperature and is identified as a diffusion mechanism [35].

The adsorption capacity is higher for materials with a larger specific surface area and a larger pore size due to the larger pore volume [36]. When pores are formed, the sorption capacity for oil and petroleum products increases. However, under the influence of temperature, the porous structure can be partially degraded. As a result, this can lead to a decrease in sorption capacity [37]. The obtained results indicate that the use of too high calcination temperatures may result in obtaining a material with too small a pore diameter, which can limit the diffusion of adsorbates. Lower calcination temperatures make it possible to obtain a higher specific surface area, volume and pore size. As a result, such material can serve as a sorbent for industrial applications.

### 3.6. Thermal analysis

Figure 6 presents the results of thermal analysis showing the changes occurring in the granulated diatomite

(0.5-3 mm) during heating from ambient temperature to 1000°C.

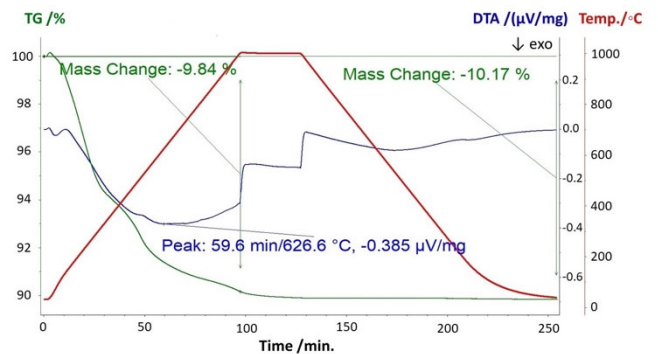


Fig. 6. Thermal decomposition of granulated diatomite: thermogravimetric (TG) and differential thermal analysis (DTA) curves

Optimization of the calcination temperature in terms of the sorption properties of petroleum substances was carried out. The curve represents changes in the material (heating effects). The greatest mass loss (9.84%) was observed up to 100 minutes of measurement. This is reflected in the recorded DTA curve and the determined extreme of the exothermic effect at 626.6°C. The total mass loss was 10.17%. The initial mass loss from an ambient temperature of about 200°C can be attributed to the loss of water absorbed in the diatomaceous earth [28]. Another mass loss, up to a temperature of about 630°C, may be due to the fact that dehydroxylation of some silanol groups [28] and combustion of organic matter [9] occur on the outer surface of the diatomite. The next range, from 630°C to 1000°C, shows less mass loss, indicating kaolinite degradation and impurities [5].

The particle size of diatomite does not affect the calcination temperature but is important in choosing a measurement method.

### 3.7. Absorption capacity of diatomite aggregate

Figure 7 shows the results of the effect of calcination temperature on the absorption capacity of diatomite aggregate.

Diatomite aggregate with a gradation of 0.9-0.4 mm in the delivery condition (DC) had an absorption capacity of 48%. Importantly, the calcination process increased the absorption capacity of the material. The result depended on the calcination temperature used. The lowest increase in absorbency was recorded at a treatment temperature of 850°C, where the diatomite aggregate reached an

absorbency of 66%. Thereafter, the absorption capacity of the material increased by another 2% each time for diatomite calcined at 650°C and 750°C reaching 68% and 70%, respectively. Treatment at 600°C yielded a slightly higher result, at 71%. Significantly, the use of a calcination temperature of 1000°C succeeded in obtaining a sorbent with an absorption capacity of 77%. In the temperature range from 650°C to 850°C, the absorption capacity was stabilized, which can be attributed to partial and early vitrification of the material [1]. The adsorption capacity of diatomite in the delivery condition and after the calcination process was found to be negatively correlated with their specific surface area (Tab. 5). As the specific surface area of the absorbents decreases, their absorption capacity increases.

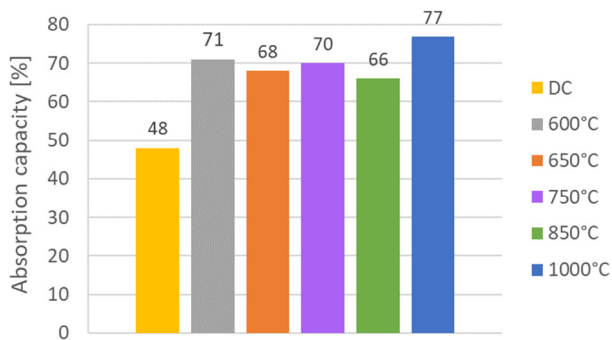


Fig. 7. Effect of calcination temperature of aggregate with grain gradation of 0.9-0.4 mm on the absorption capacity of diatomite aggregate

Zhao et al. [12] in their work also observed that the absorption capacity of diatomite increases with increasing activation temperature. Similarly, Ilia et al. [1] noted in their work that there was an increase in absorption capacity in heated samples (at 400°C, 670°C and 850°C) compared to raw materials. They also observed that the absorption capacity was either reduced or stabilized in the temperature range from 670°C to 800°C.

The results clearly indicate that calcined diatomite is suitable for use as an absorption material for industrial applications. Currently used sorbents have an absorption efficiency of up to 60-70% [1].

### 3.8. The effect of diatomite addition on the water absorption of concrete

The results of testing the effect of diatomite on the water absorption of concrete are shown in Figure 8.

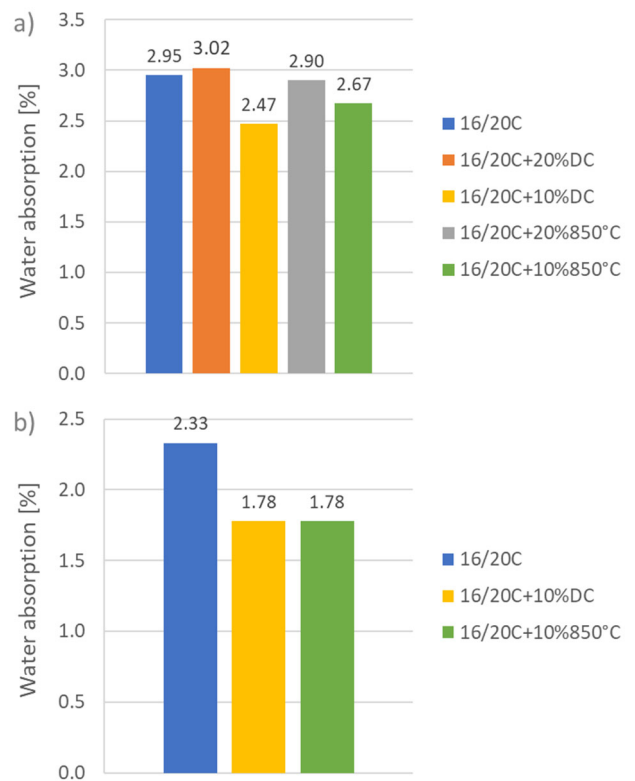


Fig. 8. The effect of diatomite on the water absorption of concrete for specimens with dimensions: a) 50×50×50 mm; b) 150×150×150 mm

The results obtained from the concrete water absorption tests present that the samples without the addition of diatomite (16/20C) with dimensions of 50×50×50 mm show a water absorption of 2.95%. The addition of diatomite in the delivery condition (DC) in the amount of 20% resulted in a slight increase in water absorption (to a value of 3.02%). However, a decrease in water absorption was recorded for the remaining samples with diatomite addition. The largest decrease occurred for samples with 10% diatomite, both in the delivery condition (2.47%) and calcined at 850°C (2.67%). For this reason, these two variants were selected for the water absorption tests conducted on 150×150×150 mm samples, as they had the lowest water absorption. They were then compared with samples made without the addition of diatomite (16/20C). For samples made in 150×150×150 mm moulds (Fig. 8b), the absorbability was lower than for samples made in 50×50×50 mm moulds (Fig. 8a). Comparing the samples without and with the addition of diatomite; it can be seen that the addition of diatomaceous earth caused a decrease in absorbability from 2.33% to 1.78% (both for diatomite in the delivery condition and after calcination process).



The results of Ergün et al. [38] showed that adding 10% diatomite resulted in higher flexural strength and compressive strength of concrete. From an ecological and economic point of view, replacing cement with diatomite can improve the mechanical properties of concrete mixtures [38,39].

#### 4. Conclusions

This study aimed to demonstrate the applicability of diatomite derived from the Carpathian Foothills. It was proved that diatomite is a safe raw material that can be used as a sorbent of petroleum substances. Based on the research, the following statements were made:

- The calcination process has a significant effect on the particle morphology, chemical composition and specific surface area of diatomaceous earth.
- Sorption of petroleum substances of the tested diatomite was 77%. In contrast, currently used sorbents have an absorption efficiency of up to 60-70%.
- Water absorption tests showed that a 10% addition of diatomaceous earth to concrete reduces the water absorption of samples by 23%.
- The chemical composition of diatomite suggests its high potential for use in the synthesis of geopolymers. This is important from both an environmental and economic point of view.

#### Acknowledgements

This work has been financed by the National Centre for Research and Development in Poland under the grant: „Development and demonstration of technologies for the production of highly effective diatomite-based sorbents and diatomite fillers” realized within the project 1/4.1.4/2020 funded by the National Centre for Research and Development, Project No.: POIR.04.01.04-00-0032/20.

#### References

- [1] I. Ilija, M. Stamatakis, T. Perraki, Mineralogy and technical properties of clayey diatomites from north and central Greece, *Open Geosciences* 1/4 (2009) 393-403. DOI: <https://doi.org/10.2478/v10085-009-0034-3>
- [2] A.A. Sharipova, S.B. Aidarova, N.Y. Bekturganova, A. Tleuova, M. Kerimkulova, O. Yessimova, T. Kairaliyeva, O. Lygina, S. Lyubchik, R. Miller, Triclosan adsorption from model system by mineral sorbent diatomite, *Colloids Surfaces A* 532 (2017) 97-101. DOI: <https://doi.org/10.1016/j.colsurfa.2017.06.012>
- [3] E. Gulturk, M. Guden, Thermal and acid treatment of diatom frustules, *Journal of Achievements in Materials and Manufacturing Engineering* 46/2 (2011) 196-203.
- [4] M. Pavlíková, P. Rovnaníková, M. Záleská, Z. Pavlík, Diatomaceous Earth—Lightweight Pozzolanic Admixtures for Repair Mortars—Complex Chemical and Physical Assessment, *Materials* 15/19 (2022) 6881. DOI: <https://doi.org/10.3390/ma15196881>
- [5] M.T. Phong, T.D.M. Dang, Preparation of filter aids based on Lam Dong diatomite, *Vietnam Journal of Science and Technology* 50/1 (2017) 63-71. DOI: <https://doi.org/10.15625/0866-708X/50/1/9473>
- [6] A. Šaponjić, M. Stanković, J. Majstorović, B. Matović, S. Ilić, A. Egelja, M. Kokunešoski, Porous ceramic monoliths based on diatomite, *Ceramics International* 41/8 (2015) 9745-9752. DOI: <https://doi.org/10.1016/j.ceramint.2015.04.046>
- [7] Z. Lv, A. Jiang, J. Jin, Influence of ultrafine diatomite on cracking behavior of concrete: an acoustic emission analysis, *Construction and Building Materials* 308 (2021) 124993. DOI: <https://doi.org/10.1016/j.conbuildmat.2021.124993>
- [8] M. Lutyński, P. Sakiewicz, S. Lutyńska, Characterization of diatomaceous earth and halloysite resources of Poland, *Minerals* 9/11 (2019) 670. DOI: <https://doi.org/10.3390/min9110670>
- [9] A.A. Reka, B. Pavlovski, E. Fazlija, A. Berisha, M. Pacarizi, M. Daghmechi, C. Sacalis, G. Jovanovski, P. Makreski, A. Oral, Diatomaceous Earth: Characterization, thermal modification, and application, *Open Chemistry* 19/1 (2021) 451-461. DOI: <https://doi.org/10.1515/chem-2020-0049>
- [10] Y. Gao, Y. Han, W. Li, Flotation behavior of diatomite and albite using dodecylamine as a collector, *Minerals* 8/9 (2018) 371. DOI: <https://doi.org/10.3390/min8090371>
- [11] M. Nazhipkyzy, R.R. Nemkayeva, A. Nurgain, A.R. Seitkazinova, B.K. Dinistanova, A.T. Issanbekova, N. Zhylybayeva, N.S. Bergeneva, G.U. Mamatova, The Use of Diatomite as a Catalyst Carrier for the Synthesis of Carbon Nanotubes, *Nanomaterials* 12/11 (2022) 1817. DOI: <https://doi.org/10.3390/nano12111817>
- [12] Y.H. Zhao, J.T. Geng, J.C. Cai, Y.F. Cai, C.Y. Cao, Adsorption performance of basic fuchsin on alkali-activated diatomite, *Adsorption Science and Technology* 38/5-6 (2020) 151-167. DOI: <https://doi.org/10.1177/0263617420922084>

- [13] M.A.M. Khraisheh, M.S. Alg-Houti, Enhanced Dye Adsorption by Microemulsion-Modified Calcined Diatomite ( $\mu\text{E-CD}$ ), *Adsorption* 11 (2005) 547-559. DOI: <https://doi.org/10.1007/s10450-005-5612-5>
- [14] Z. Ren, Y. He, R. Zheng, Z. Guo, H. Gao, X. He, F. Wu, X. Ji, The preparation and characterization of calcined diatomite with high adsorption properties by CaO hydrothermal activation, *Colloids Surfaces A* 636 (2022) 128134. DOI: <https://doi.org/10.1016/j.colsurfa.2021.128134>
- [15] X. Li, H. Lin, H. Jiang, Y. Zhang, B. Liu, Y. Sun, C. Zhao, Preparation and properties of a new bio-based epoxy resin/diatomite composite, *Polymer Degradation and Stability* 187 (2021) 109541. DOI: <https://doi.org/10.1016/j.polymdegradstab.2021.109541>
- [16] D. Taoukil, Y. El meski, M. Ihassane Lahlaouti, R. Djedjig, A. El bouardi, Effect of the use of diatomite as partial replacement of sand on thermal and mechanical properties of mortars, *Journal of Building Engineering* 42 (2021) 103038. DOI: <https://doi.org/10.1016/j.jobbe.2021.103038>
- [17] X. Li, J.G. Sanjayan, J.L. Wilson, Fabrication and stability of form-stable diatomite/paraffin phase change material composites, *Energy and Buildings* 76 (2014) 284-294. DOI: <https://doi.org/10.1016/j.enbuild.2014.02.082>
- [18] S.D. Mustafov, F. Sen, M.O. Seydibeyoglu, Preparation and characterization of diatomite and hydroxyapatite reinforced porous polyurethane foam biocomposites, *Scientific Reports* 10 (2020) 13308. DOI: <https://doi.org/10.1038/s41598-020-70421-3>
- [19] N. Turkten, A novel low-cost photocatalyst: preparation, characterization, and photocatalytic properties of CeO<sub>2</sub>-diatomite composites, *Water* 14/21 (2022) 3373. DOI: <https://doi.org/10.3390/w14213373>
- [20] T. Sinsiri, T. Phoo-ngernkham, V. Sata, P. Chindapasirt, The effects of replacement fly ash with diatomite in geopolymer mortar, *Computers and Concrete* 9/6 (2012) 427-437. DOI: <https://doi.org/10.12989/cac.2012.9.6.427>
- [21] C. Bagci, G.P. Kutyla, W.M. Kriven, Fully reacted high strength geopolymer made with diatomite as a fumed silica alternative, *Ceramics International* 43/17 (2017) 14784-14790. DOI: <https://doi.org/10.1016/j.ceramint.2017.07.222>
- [22] K. Şahbudak, Mechanical and Thermal Evaluation of Diatomite Doped Fly Ash Based Geopolymers, *Materials Science (Medžiagotyra)* 28/1 (2022) 75-81. DOI: <https://doi.org/10.5755/j02.ms.26796>
- [23] A. Font, L. Soriano, L. Reig, M.M. Tashima, M.V. Borrachero, J. Monzó, J. Payá, Use of residual diatomaceous earth as a silica source in geopolymer production, *Materials Letters* 223 (2018) 10-13. DOI: <https://doi.org/10.1016/j.matlet.2018.04.010>
- [24] Z. Ahmadi, J. Esmaceli, J. Kasaei, R. Hajialioghli, Properties of sustainable cement mortars containing high volume of raw diatomite, *Sustainable Materials and Technologies* 16 (2018) 47-53. DOI: <https://doi.org/10.1016/j.susmat.2018.05.001>
- [25] J. Fang, Y. Wang, K. Wang, W. Dai, Y. Yu, C. Li, Experimental Study on the Mechanical Properties of Diatomite-Modified Coarsal Cement Soil, *Materials* 15/21 (2022) 7857. DOI: <https://doi.org/https://doi.org/10.3390/ma15217857>
- [26] Górttech Sp. z o.o., Safety Data Sheet - DIATO: diatomite sorbent, 2018 (in Polish). Available from: [https://diato.pl/wp-content/uploads/2017/10/Karta\\_charakterystyki\\_sorbentu\\_diatomitowy.pdf](https://diato.pl/wp-content/uploads/2017/10/Karta_charakterystyki_sorbentu_diatomitowy.pdf)
- [27] T. Węsierski, O. Eszer, Determining the Components of Foaming Agents That Can Have a Decisive Impact On Reducing the Absorption Properties of Rigid Polyurethane Foam Waste in Relation to Post-Foaming Waste, *Safety and Fire Technology* 50/2 (2018) 50-62. DOI: <https://doi.org/10.12845/bitp.50.2.2018.4>
- [28] A. Chaisena, K. Rangsrivatananon, Effects of thermal and acid treatments on some physico-chemical properties of Lampang diatomite, *Journal of Science Technology* 11 (2004) 289-299.
- [29] W. Aguilar-Mamani, G. García, J. Hedlund, J. Mouzon, Comparison between leached metakaolin and leached diatomaceous earth as raw materials for the synthesis of ZSM-5, *SpringerPlus* 3 (2014) 292. DOI: <https://doi.org/10.1186/2193-1801-3-292>
- [30] B. Figarska-Warchoł, M. Rembiś, G. Stańczak, The impact of calcination on changes in the physical and mechanical properties of the diatomites of the Leszczawka Member (the Outer Carpathians, Poland), *Geology, Geophysics and Environment* 45/4 (2019) 269. DOI: <https://doi.org/10.7494/geol.2019.45.4.269>
- [31] J. Marczyk, C. Ziejewska, S. Gądek, K. Korniejenko, M. Łach, M. Góra, I. Kurek, N. Dogan-Saglamtimur, M. Hebda, M. Szechyńska-Hebda, Hybrid materials based on fly ash, metakaolin, and cement for 3D printing, *Materials* 14/22 (2021) 6874. DOI: <https://doi.org/10.3390/ma14226874>
- [32] M. Łach, A. Greła, K. Pławecka, M.D. Guigou, J. Mikula, N. Komar, T. Bajda, K. Korniejenko, Surface Modification of Synthetic Zeolites with Ca and HDTMA Compounds with Determination of Their Phytoavailability and Comparison of CEC and AEC Parameters, *Materials* 15/12 (2022) 4083. DOI: <https://doi.org/10.3390/ma15124083>

- [33] H. Tang, X. Xu, B. Wang, C. Lv, D. Shi, Removal of ammonium from swine waste water using synthesized zeolite from fly ash, *Sustain* 12/8 (2020) 3423. DOI: <https://doi.org/10.3390/SU12083423>
- [34] L. Xiao, B. Pang, Experimental study on the effect of calcination on the volcanic ash activity of diatomite, *IOP Conference Series: Materials Science and Engineering* 231 (2017) 012089. DOI: <https://doi.org/10.1088/1757-899X/231/1/012089>
- [35] S. Bailliez, A. Nzihou, The kinetics of surface area reduction during isothermal sintering of hydroxyapatite adsorbent, *Chemical Engineering Journal* 98/1-2 (2004) 141-152. DOI: <https://doi.org/10.1016/j.cej.2003.07.001>
- [36] C.L. Mangun, M.A. Daley, R.D. Braatz, J. Economy, Effect of pore size on adsorption of hydrocarbons in phenolic-based activated carbon fibers, *Carbon* 36/1-2 (1998) 123-129. DOI: [https://doi.org/10.1016/s0008-6223\(97\)00169-3](https://doi.org/10.1016/s0008-6223(97)00169-3)
- [37] I.L. Rogovskii, O.M. Kalivoshko, K. Yu Maksimovich, E. Yu Maksimovich, Research of Mixed Carbon Sorbents for Removal of Oil Products from Water and Soil for Preservation of Environmental Infrastructure, *IOP Conference Series: Earth and Environmental Science* 720 (2021) 012108. DOI: <https://doi.org/10.1088/1755-1315/720/1/012108>
- [38] A. Ergün, Effects of the usage of diatomite and waste marble powder as partial replacement of cement on the mechanical properties of concrete, *Construction and Building Materials* 25/2 (2011) 806-812. DOI: <https://doi.org/10.1016/j.conbuildmat.2010.07.002>
- [39] N. Sharma, M. Singh Thakur, P.L. Goel, P. Sihag, A review: Sustainable compressive strength properties of concrete mix with replacement by marble powder, *Journal of Achievements in Materials and Manufacturing Engineering* 98/1 (2020) 11-23. DOI: <https://doi.org/10.5604/01.3001.0014.0813>



© 2022 by the authors. Licensee International OCSCO World Press, Gliwice, Poland. This paper is an open access paper distributed under the terms and conditions of the Creative Commons Attribution-NonCommercial-NoDerivatives 4.0 International (CC BY-NC-ND 4.0) license (<https://creativecommons.org/licenses/by-nc-nd/4.0/deed.en>).